Mechanical and Thermal Characterization of Additively Manufactured Carbon/Nylon 12 and Carbon/PEEK Composites

Matik Heskin, Bradley Deuser, Thomas Schuman and K. Chandrashekhara*

Missouri University of Science and Technology, Rolla, MO 65409, USA

John Bayldon and Jeff DeGrange

Impossible Objects Inc., Northbrook, IL 60062, USA

Steven Patterson and Neiko Levenhagen

Department of Energy's Kansas City National Security Campus**, Kansas City, MO 64147, USA

*Author for correspondence: chandra@mst.edu

**The Department of Energy's Kansas City National Security Campus is operated and managed by Honeywell Federal Manufacturing Technologies, LLC under contract number DE-NA0002839

Abstract

This study explores additive manufacturing of carbon fiber-reinforced thermoplastic composites using the Composite-Based Additive Manufacturing (CBAM) process. Carbon/Nylon 12 and Carbon/PEEK composites were fabricated and evaluated through mechanical (compression, tensile, flexural, and impact) and thermal (DSC and TGA) tests. Carbon/PEEK exhibited superior mechanical performance, with 97.5% higher tensile strength, 79.8% higher elastic modulus, and 59.6% higher flexural strength compared to Carbon/Nylon 12. Thermal testing showed that Carbon/PEEK had higher thermal stability, beginning degradation at 350°C versus 298°C for Carbon/Nylon. These results indicate that CBAM-fabricated Carbon/PEEK composites are suitable for applications requiring high strength and temperature resistance.

1. Introduction

Additive Manufacturing (AM) has been increasingly used for the fabrication of end products. The ability of additive manufacturing process to reduce manufacturing costs and lead times is of great interest to the composite manufacturing industry [1-5]. Fused deposition modelling (FDM) is presently one of the most popular thermoplastic additive manufacturing techniques due to its easy operation and reproducibility [6-7]. The parts are manufactured by melting and extruding the polymeric filament onto a base plate through a heated nozzle in a predefined pattern. It uses layer-

by-layer deposition of a melted thermoplastic filament. The extruded polymeric material cools down in the chamber and melds with the adjacent materials [8].

Complex shaped materials that are difficult to produce with traditional manufacturing processes can be built by sequential deposition. Hollow structures can be designed and built which possess adequate mechanical strength while offering significant weight savings. Additive manufacturing of complex shapes has lower ecological impact and material waste compared to traditional machining processes [9]. Between all additive manufacturing methods almost any material can be used; thermoplastics [10-11], thermosets [12-13], metals [14-15], and ceramics [16] are, if not already in common use, at least possible using additive manufacturing.

Of the thermoplastics in use, nylon has already shown great use throughout industry [17,18]. Nylon is commonly used in FDM printing due to its lower melt temperature and moderate mechanical properties. Polyether ether ketone (PEEK) is used less frequently in additive manufacturing due to its high melt temperature and chemical inertness [19-21] which can make manufacturing difficult but has significant advantages in applications where temperature stability is critical.

Within extrusion-based AM some significant work has already been done regarding fiber addition, primarily with FDM [22] and injection molding [23]. However, integration of fibers in polymers commonly lack critically defined aspects such as the application of temperature and pressure required to achieve proper thermo-mechanical consolidation and non-uniform temperature fields promoting process-induced defects. Benefits to temperature and pressure application include lowered porosity and increased mechanical properties [24]. In the present study the Composite Based Additive Manufacturing (CBAM) process of Impossible Objects Inc. is used to manufacture Carbon/PEEK and Carbon/Nylon 12 thermoplastic composite parts.

Previous work on CBAM at Missouri S&T included creating Carbon/PEEK tool plates for injection molding process [25]. The CBAM process is currently only applicable for thermoplastic composites though ongoing projects at Missouri S&T are focused on expanding the use of CBAM to thermoset applications. While additive manufacturing of thermoplastic composites has been studied using methods like FDM and injection molding, relatively few studies have looked at the mechanical and thermal properties of composites made with the CBAM process. CBAM offers several advantages over filament-based printing, especially in terms of fiber architecture, layer bonding, and design flexibility. Recent work has shown growing interest in fiber-reinforced additive manufacturing, including techniques like coextrusion and binder-jet processes, but full property characterization of CBAM parts remains limited [26]. Other studies have reported high strength values in PEEK-based composites using continuous fiber reinforcement, with tensile strengths exceeding 500 MPa [27], but these often require more complex or less flexible processing routes. The present work helps fill this gap by comparing the mechanical and thermal behavior of CBAM-fabricated Carbon/PEEK and Carbon/Nylon 12 composites, providing a baseline for future high-performance applications.

2. Additive Manufacturing

2.1 Materials

The materials used for this study include randomly oriented carbon fiber sheets and powder-based PEEK and Nylon 12 thermoplastic polymers, all of which were directly acquired from Impossible Objects. The PEEK and Nylon powders both have a purity of 99% or greater. Tabulated compressive strengths for Nylon 12 and PEEK are 75 MPa [28] and 124 MPa [29] respectively, though reported values for Nylon 12 vary significantly.

Carbon/PEEK and Carbon/Nylon 12 were selected for this study due to their availability in powder form from Impossible Objects and their compatibility with the CBAM process. Nylon 12 offers ease of processing due to its lower melt temperature, while PEEK provides high-temperature stability and mechanical strength. Nylon 12 is generally recognized to have lower moisture absorption and better dimensional stability compared to Nylon 6 or 6,6, making it more suitable for applications involving variable environmental conditions [30]. These materials also represent a performance range, allowing comparison of a high-strength, high-temp polymer (PEEK) against a more accessible engineering plastic (Nylon 12). In contrast to compression or injection molding, CBAM enables direct fabrication of complex geometries with continuous fiber reinforcement and reduced tooling needs. Additionally, Impossible Objects does not currently offer Nylon 6 or 6,6 for use with the CBAM process, so these materials were not available for evaluation.

The randomly oriented carbon fibers used for this study had a density of 17 g/m^2, were 0.25 mm thick, and had a relatively high sizing content of 10% polymer binder. Average fiber length is 12.7 mm as reported by Impossible Objects. No independent validation of fiber length was performed for this study. The average fiber volume fraction was approximately 25.72% and 18.67% for Carbon/Nylon 12 and Carbon/PEEK respectively. Similarly, porosity for Carbon/Nylon 12 and Carbon/PEEK is 25.35% and 26.431% respectively [31]. These values are based on acid digestion testing completed in past work. While the hot press process consolidates the manufactured components, porosity is primarily a result of insufficient powder deposition. The CBAM process is currently incapable of depositing thick enough powder layers to sufficiently fill voids in and between lamina. Ongoing studies have reported a 10% reduction in porosity for these materials. Newer CBAM machines from Impossible Objects have lessened, but not eliminated, porosity in AM components.

The carbon fiber sheets used in this study consist of fibers that are randomly oriented within the plane of the sheet (2D random orientation). This distribution is inherent to the sheets provided by Impossible Objects. In-plane random orientation was confirmed by visual inspection (See Figure 5) during sample preparation, with no significant through-thickness fiber alignment observed.

2.2 Manufacturing of the AM composites

Carbon/Nylon 12 and Carbon/PEEK specimens for the present study were designed per ASTM standards [32-35] using CBAM equipment. An outline of the manufacturing process can be found in Figure 1 and a supplementary video created by Impossible Object can be found in Reference [36].

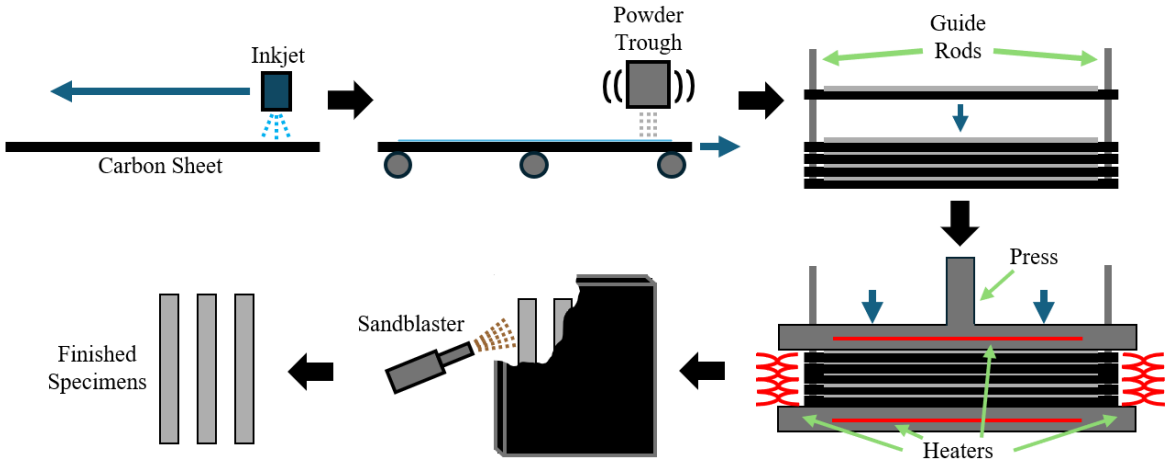

Figure 1: CBAM Processing Cycle

The printing process for CBAM is as follows. A 3D model is split into several layers based on the final thickness of one cured fiber/polymer composite sheet. The sliced model is fed through proprietary software to the CBAM machine. The Inkjet heads of the machine deposit a liquid binder on the surface of the carbon fiber sheet in the desired pattern. The desired polymer powder is held in a metal trough with a thin long slit at the bottom. The polymer is waterfalled on to the surface of the sheet as the trough vibrates. The powder sticks to the printed binder while the rest of the loose powder is vacuumed away. The printed sheets are stacked on top of each other until all layers have been primed.

Once the printing is complete, the sheets are hot pressed following a heat and pressure cycle dependent on the type of polymer used. Specifically, the respective stacks are brought up to and held at the melting temperature of Nylon 12 or PEEK powder while under slight (< 50lbs.) pressure for 10 minutes before being compressed to their final height. The recommended press cycles for PEEK and Nylon 12 are shown in Figure 2. Ramp rate was governed by the max rate attainable by

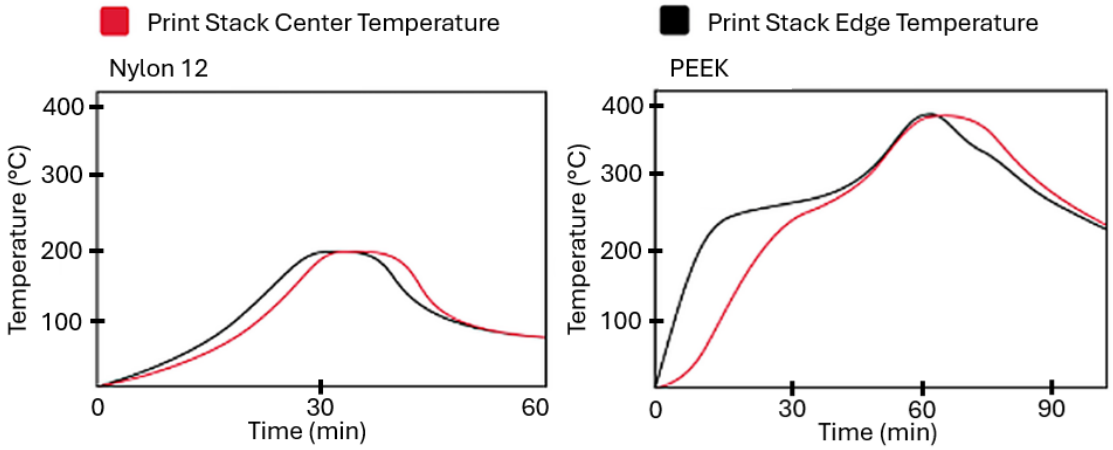

Figure 2: General Hot Press Cycles for PEEK and Nylon 12 (Impossible Objects Inc.)

the hot press and varies between 4-6 °C/min. Due to possible temperature runaway between the center and edges of a stack during high temperature processing, PEEK hot pressing utilizes thermocouples placed through the stack in predetermined unprinted areas, and in-situ temperatures are monitored during the entire cycle. A modification to a general heating cycle, the hold seen in the PEEK hot press cycle (Figure 2) helps the build reach a common temperature before heating to the full melt temperature, decreasing the chance of a failed print.

All test specimens were removed from pressed CBAM sheet stacks. Specimens were extracted by sandblasting unbound fibers away using a 50/50 alumina and walnut shell powder mix. As refined and recommended by Impossible Objects, a nozzle pressure of no greater than 40 psi was used to avoid removing or damaging any bound fibers/matrix, allowing specimens to retain their as-printed dimensions and shape. All specimens were cut along the primary build direction, with loading applied parallel to the in-plane fiber orientation of each printed sheet. Due to the CBAM process using stacked sheets with no preferential in-plane fiber alignment, this represents an average in-plane response. Testing in the through-thickness direction was not performed, but future work may explore directional dependency more thoroughly. These materials are expected to exhibit predominantly matrix-dominated material properties in the through-thickness directions..

Print limitations of the CBAM process are primarily related to minimum feature size. Features smaller than 1 mm are generally well-printed but susceptible to damage during sandblasting. Overhangs, which pose difficulties in standard FDM printing, are effectively supported during CBAM printing. CBAM manufacturing is capable of printing complete 90-degree overhangs as deposited powder is always supported by surrounding unbound fiber.

Figure 3 shows the Carbon/PEEK AM printed compression, flexural, and tensile test samples. Figure 4 shows the Carbon/PEEK impact specimens. Carbon/Nylon 12 specimens are visually near-indistinguishable from the Carbon/PEEK parts.

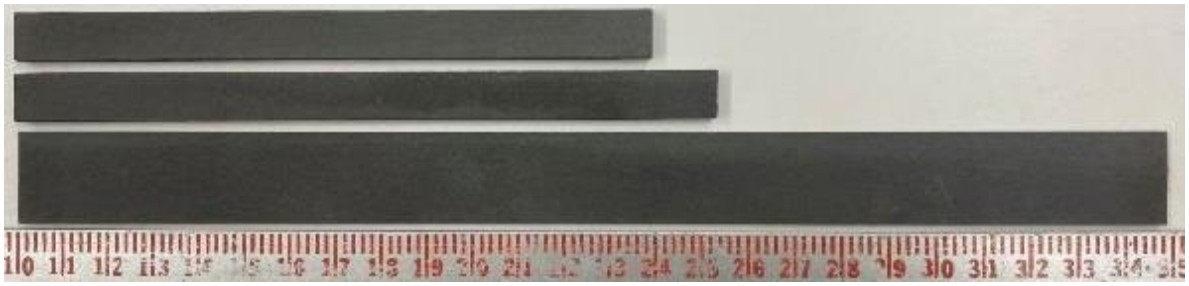

Figure 3: Carbon/PEEK Compression (Top), Flexural (Middle) and Tensile (Bottom) Flat Samples

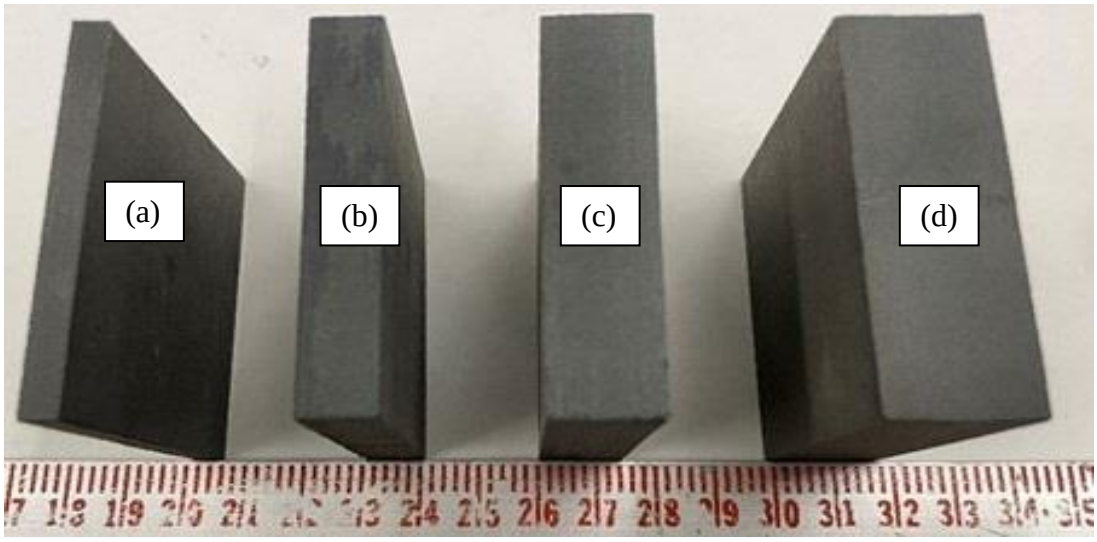

Figure 4: Carbon/PEEK (a) 5 mm, (b) 10 mm, (c) 15 mm, and (d) 20 mm Thick Impact Samples

Optical microscopy of the X-Y plane (in-plane) was completed on two representative samples of Carbon/Nylon 12 and Carbon/PEEK, as shown in Figure 5. The randomly orientated fibers are clearly visible, and visible porosity are common throughout the cross section.

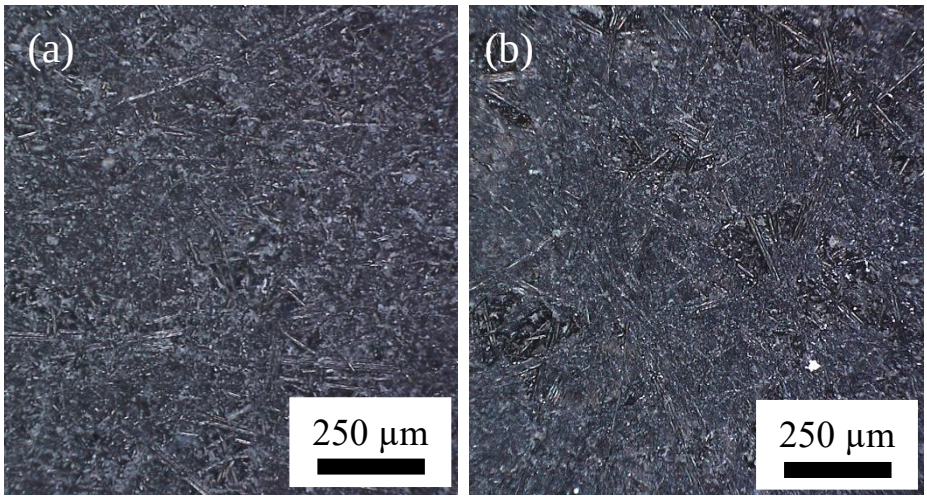

Figure 5: Optical Microscopy of (a) Carbon/Nylon 12 and (b) Carbon/PEEK

3. Performance Evaluation

The performance of the Carbon/PEEK and Carbon/Nylon 12 composites have been evaluated based on mechanical tests, whose test matrix is seen in Table 1, and thermal testing (DSC/TGA). All mechanical and thermal tests were conducted following relevant ASTM standards. The selected tests collectively characterize the capabilities and performance limits of the evaluated materials. Between compression, tensile, and flexural testing the common mechanical performance of Carbon/Nylon 12 and Carbon/PEEK is evaluated, while impact testing provides insight into

potential specialized applications. DSC/TGA provides a fundamental characterization of thermal performance, and while heavily reliant on the type of matrix used, still describes how these composites are affected by elevated temperatures environments.

All mechanical tests were performed at standard laboratory conditions, with ambient temperature ranging from 21–23°C. Although specific humidity measurements were not recorded during testing, relative humidity in the laboratory environment was estimated at approximately 30% based on recent measurements. Specimens were conditioned in the laboratory environment for a minimum of 24 hours prior to testing to reduce variability due to moisture absorption. Across all mechanical tests, low variability between replicates was observed, indicating good consistency and repeatability in both sample fabrication and testing.

Table 1: Test Matrix

	Number of Samples Tested			
	Compression	**Tensile**	**Flexural**	**Impact (5, 10, 15, 20 mm)**
Carbon/Nylon 12	5	5	5	5
Carbon/PEEK	5	5	5	5

3.1 Compression Test

Compression specimens were designed per ASTM D6641. Sample dimensions were 140 mm × 13 mm × 4 mm [5.51 in × 0.51 in × 0.16 in]. Specimens are loaded between the upper and lower fixtures by means of friction, leaving a gauge section of 13 mm [.5 in] in-between fixtures as shown in Figure 6. Specimens are loaded via displacement-controlled loading, set to 1.3 mm/min. Five specimens of each, Carbon/PEEK and Carbon/Nylon 12 were tested.

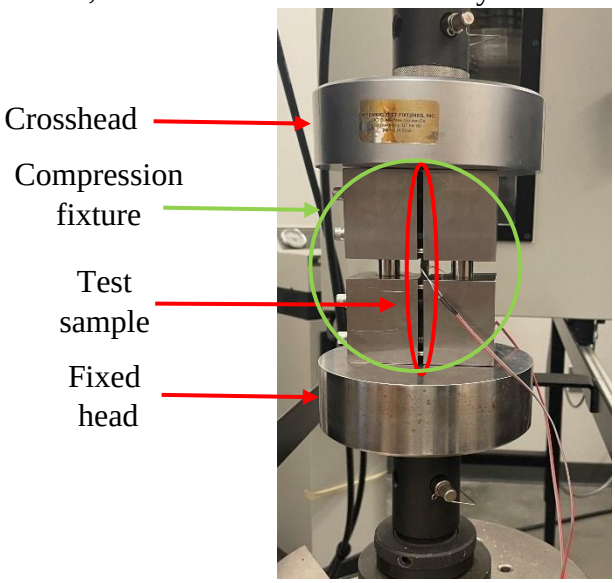

Figure 6: Compression Fixture and Sample

3.2 Tensile Test

Flat tensile specimens were designed following the test parameters defined in ASTM D3039. The sample dimensions were 250 mm × 25 mm × 2.5 mm [9.84 in × 0.98 in × 0.10 in]. An image of one of the samples used for tensile testing with the aluminum tabs can be seen below, in Figure 7(a). Two dots were added to the specimen, centered, and spaced one inch apart from each other. During testing, a camera mounted to the test platform performs digital image correlation (DIC), measuring the separation of the dots as the specimen is loaded. From this information the strain of the specimen can be determined as the test is carried out, without the need for strain gauges. Four aluminum tabs were bonded to the specimens in the gauge sections to provide a place to grip the specimen without damaging them.

All tensile testing was performed on an Instron 5985 test machine. Figure 7(b) shows a flat specimen mounted in the test machine. The red light illuminates the dots and provides better tracking for the DIC camera. The specimens were mounted in the test machine, taking care to align the edges of the aluminum tabs with the edges of the self-aligning clamps. At the start of each test, the DIC camera captures an image to confirm proper specimen placement and alignment. The image is also used to set the initial gauge length of the specimen. Per ASTM D3039, specimens were loaded under displacement-controlled loading at 5 mm/min. The test is terminated once the machine detects specimen failure. To ensure the repeatability of the test data five samples of both the Carbon/PEEK and Carbon/Nylon 12 were tested.

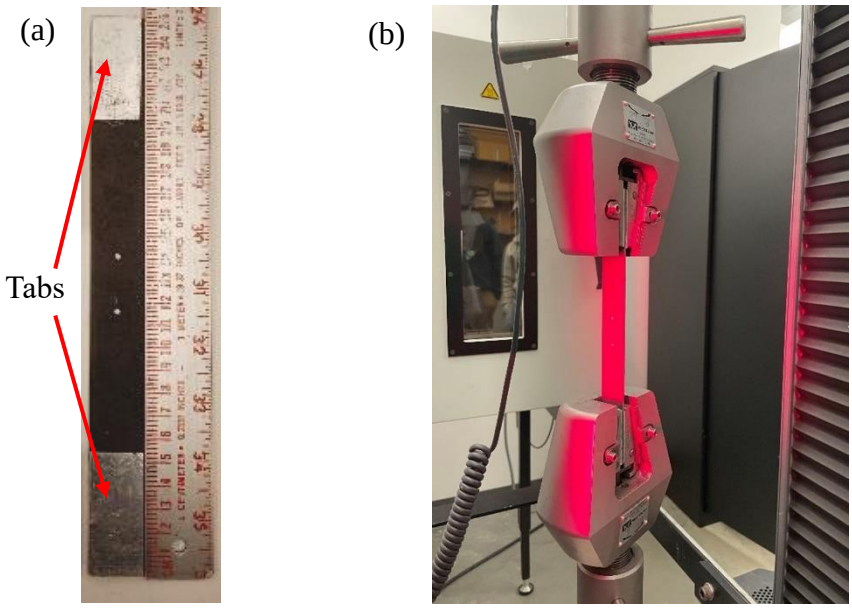

Figure 7: (a) Tensile Specimen and (b) Specimen Mounted on Instron 5895

3.3 Flexural Test

Three-point flexural testing was carried out in compliance with ASTM D7264 on an Instron 5985 test machine. The sample dimensions were 154 mm × 13 mm × 4 mm [6.06 in × 0.51 in × 0.16 in]. To maintain the span length to thickness ratio of 32:1, span length of samples was 128 mm. To ensure the repeatability of the test data five samples of both the Carbon/PEEK and Carbon/Nylon 12 were tested. The setup of the flexural sample is shown in Figure 8. Per ASTM D7264 the crosshead rate was set to 1 mm/min.

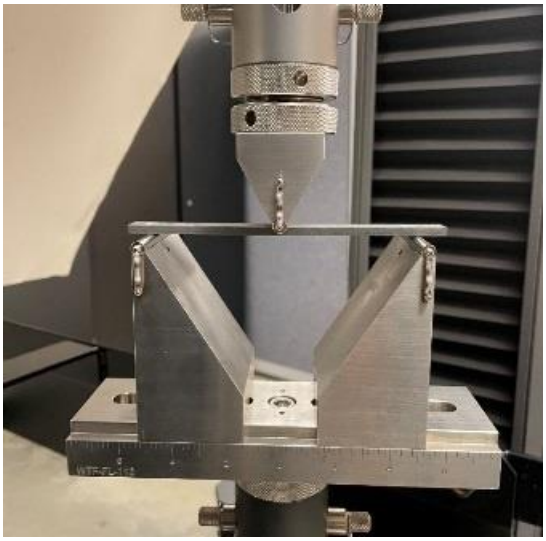

Figure 8: Flexural Sample Setup on Instron 5985

3.4 Impact Test

Low velocity impact was conducted on an Instron Dynatup 9250 HV drop tower machine in compliance with the ASTM D7136. Absorbed energy during impact was calculated automatically by the Dynatup system's energy module using force and displacement data collected throughout the impact event. The software integrates the area under the curve to determine the total energy absorbed by the specimen. This value corresponds to the difference between the initial impact energy and the rebound energy. To achieve an impact energy of 9.8 J, the drop weight was set to 6.48 kg [14.3 lbs.] and drop height was set to 154 mm [6 in]. The indenter uses a 12.7 mm [.5 in] hemispherical tip. Sample dimensions were 60 mm × 60 mm [2.36 in × 2.36 in]. Four different sample thicknesses of 5 mm, 10 mm, 15 mm, and 20 mm were tested to compare the energy absorption behavior of the Carbon/PEEK and Carbon/Nylon 12 samples. Data acquisition rate for testing was 5 MHz. The impact sample setup is shown in Figure 9.

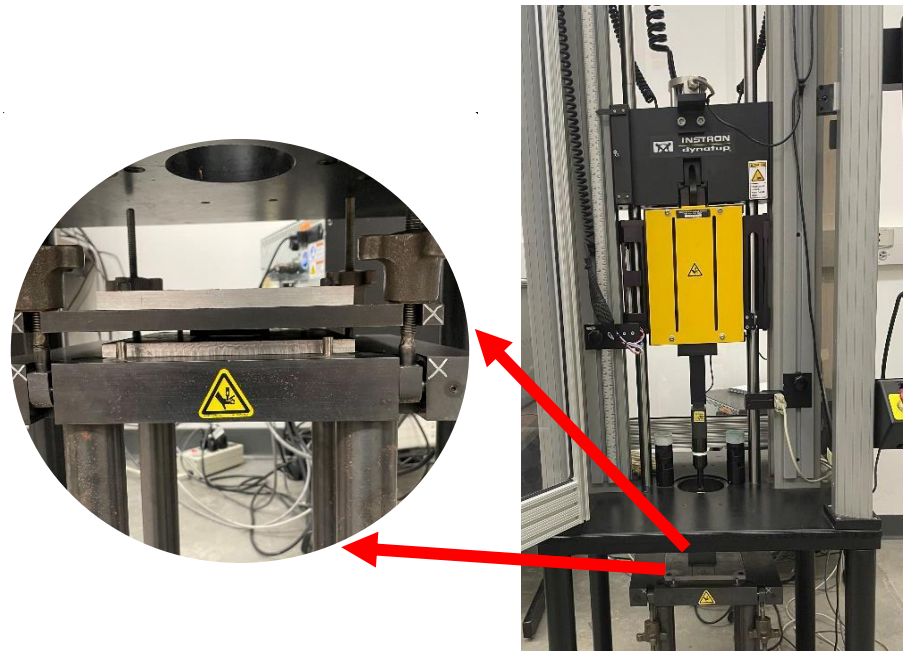

Figure 9: Impact Setup on Instron Dynatup 9250 HV

3.5 DSC/TGA

Differential scanning calorimetry (DSC) and thermogravimetric analysis (TGA) are two of the most widely used thermal analysis techniques. DSC measures the heat flow into or out of a sample as a function of temperature or time, while the sample is exposed to a controlled temperature program. TGA shows the changes in physical and chemical properties of materials as a function of increasing temperature (with constant heating rate), or as a function of time (with constant temperature and/or constant mass loss).

For the present work Netzsch STA 449 F5 Jupiter equipment was used for the DSC/TGA of Carbon/PEEK and Carbon/Nylon 12 samples. The analysis was carried out in an air and nitrogen environment using a heating rate of 5ºC/min ramp to 900ºC.

4. Results and Discussion

4.1 Compressive Test

Compressive testing is especially useful as it is a heavily matrix-dominated property. For each Carbon/PEEK and Carbon/Nylon 12 respectively, compressive strength should be close to the pure polymeric strength. Results for both composites are presented in Figure 10. The Carbon/PEEK sample showed higher maximum load and ultimate compressive strength than the Carbon/Nylon 12, nearly double in both cases. A summary of properties is shown in Table 2.

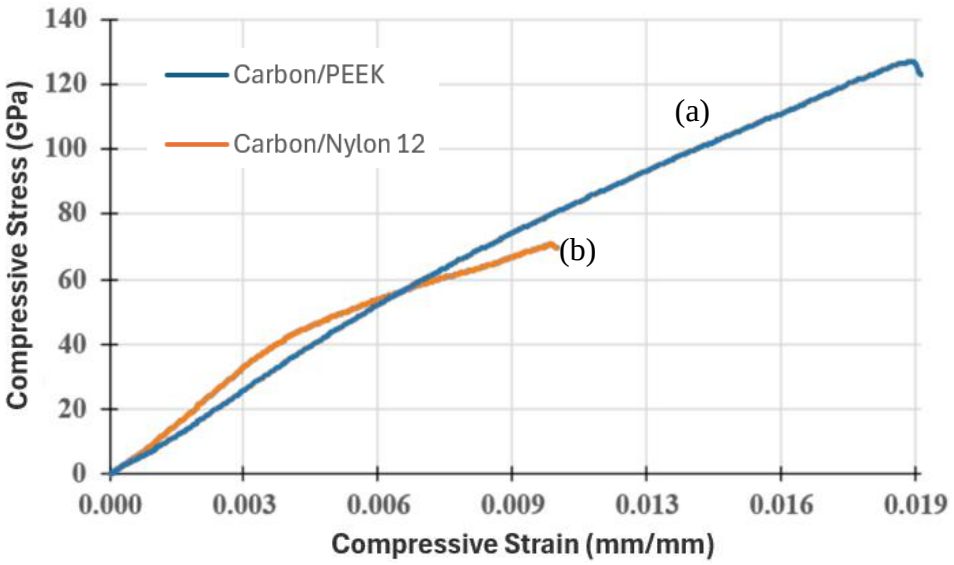

Figure 10: Compressive Tested (a) Carbon/PEEK and (b) Carbon/Nylon 12 Samples

Failure mode was very consistent between samples. Samples consistently exhibited shear failure through the thickness within the gauge section. This observation indicates sufficient interlaminar adhesion to effectively transfer loads through fibers prior to failure. An example of this failure is shown in Figure 11.

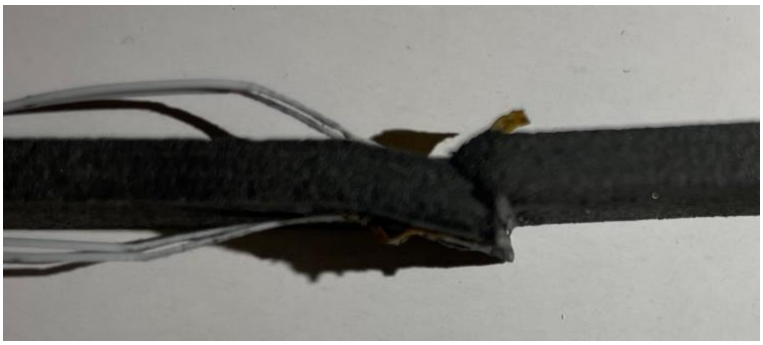

Figure 11: Failure of Compressive Specimen

Table 2: Compressive Test Data of Carbon/PEEK and Carbon/Nylon 12

Material	Maximum load (N)	Compressive strength (GPa)	Compressive modulus (GPa)
Carbon/PEEK	6615 $\pm$ 138.9	127.2 $\pm$ 7.72	6747.7 $\pm$ 411.5
Carbon/Nylon 12	3632 $\pm$ 227.6	79.60 $\pm$ 3.85	3855.1 $\pm$ 183.4

As expected, compressive strengths are very close to pure polymeric strength.

4.2 Tensile Test

The tensile tested specimens failed in two places nearly simultaneously. It is uncertain whether the samples initially failed at one location followed rapidly by another, or simultaneously at multiple locations. The current assumption is that initial failure at one location releases stored energy, subsequently causing additional fractures. This assumption is supported by the forceful nature of specimen failures observed consistently, In several cases, the central fractured segment detached and fractured further, either during free motion or upon contacting the ground.

Figure 12 shows the engineering stress vs. strain curves of Carbon/PEEK and Carbon/Nylon 12. Carbon/PEEK exhibited higher tensile strength and stiffness relative to Carbon/Nylon 12. Carbon/PEEK has approximately 97.49% higher ultimate tensile strength also the elastic modulus of Carbon/PEEK is 79.75% higher than that of Carbon/Nylon 12. Table 3 shows the Carbon/PEEK and Carbon/Nylon 12 properties attained from the tensile test.

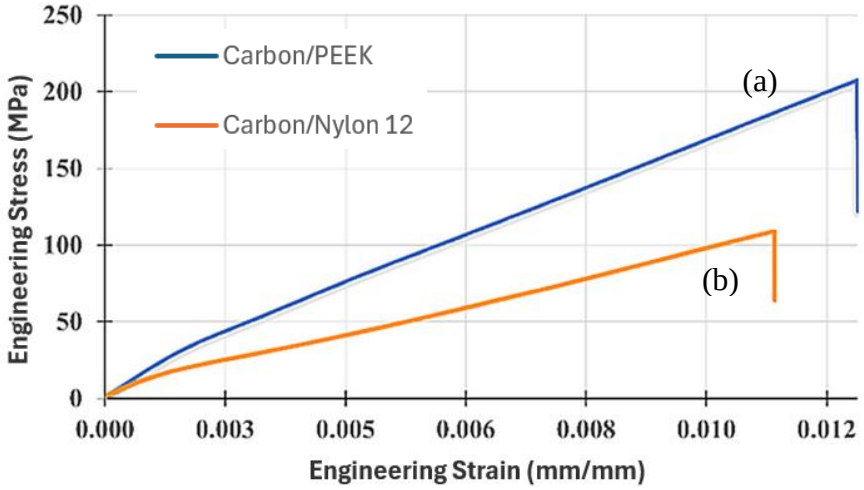

Figure 12: Engineering Stress-Strain Curve of Tensile (a) Carbon/PEEK and (b) Carbon/Nylon 12

Fractographic analysis of the tensile specimens was performed using scanning electron microscopy (SEM) to evaluate failure mechanisms and fiber–matrix interaction. Representative SEM images of the fracture surfaces, shown in Figure 13, revealed widespread fiber pullout, with many fibers partially or fully debonded from the surrounding matrix. Although only the SEM fracture surface of Carbon/PEEK is shown in Figure 13, the fracture morphology was indistinguishable from that of Carbon/Nylon 12. This indicates that tensile failure was dominated by interfacial debonding rather than fiber breakage, suggesting that the fiber–matrix adhesion was the limiting factor in load transfer. The prevalence of undamaged fiber surfaces and extraction channels further supports this case, as effective load transfer would typically result in more fiber fracture and surface roughness.

The extensive fiber pullout observed in both Carbon/PEEK and Carbon/Nylon 12 specimens also explains the relatively low elongation at break, as load was not effectively distributed across the reinforcing fibers during tensile deformation. In particular, the Carbon/PEEK samples, while

exhibiting higher tensile strength and modulus, still showed signs of imperfect bonding at the interface.

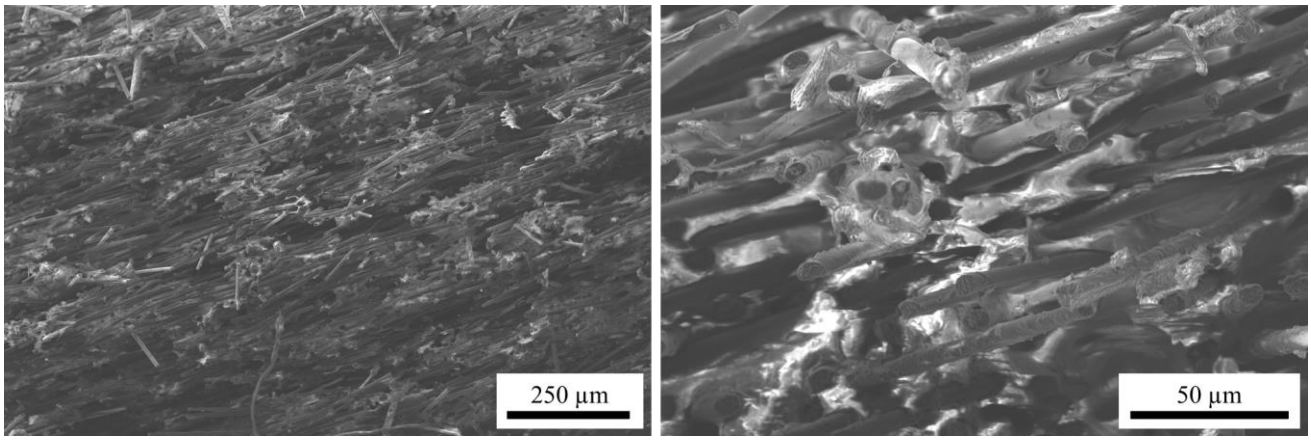

Figure 13: Fracture Surface of Carbon/PEEK Tensile Tested Samples

Table 3: Tensile Test Data of Carbon/PEEK and Carbon/Nylon 12

Material	Maximum load (N)	Ultimate tensile strength (MPa)	Elongation at break (%)	Young's modulus (GPa)
Carbon/PEEK	12897 ± 244.4	206.4 ± 3.91	1.162 ± 0.04	17.49 ± 0.73
Carbon/Nylon 12	6529 ± 471.7	104.5 ± 7.55	1.1 ± 0.001	9.73 ± 0.23

The tensile strength of our CBAM-fabricated Carbon/PEEK composites was measured at 206.4 MPa, nearly double the 115 MPa strength reported for a set of FDM printed Carbon/PEEK composites [37]. This suggests that the CBAM process can achieve mechanical properties on par with or exceeding those obtained through FDM printed composites.

4.3 Flexural Test

Figure 14 shows the flexural tested samples. It can be observed that the samples failed from the center. This failure pattern resulted from the central loading configuration. Figure 15 shows the flexural curves for Carbon/PEEK and Carbon/Nylon 12 samples.

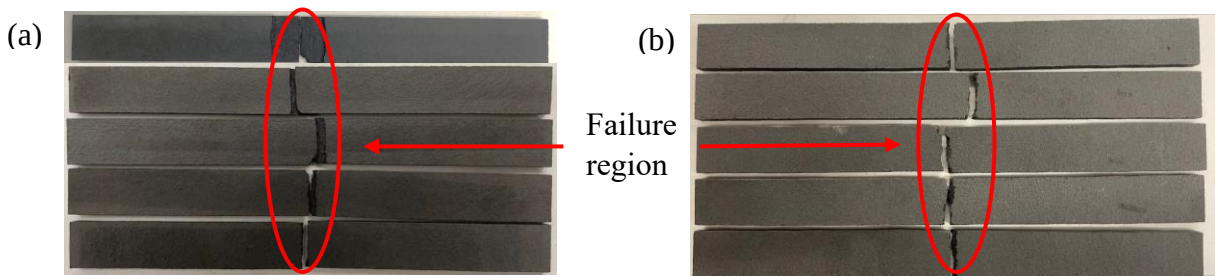

Figure 14: Carbon/Nylon 12 Flexural Tested Samples

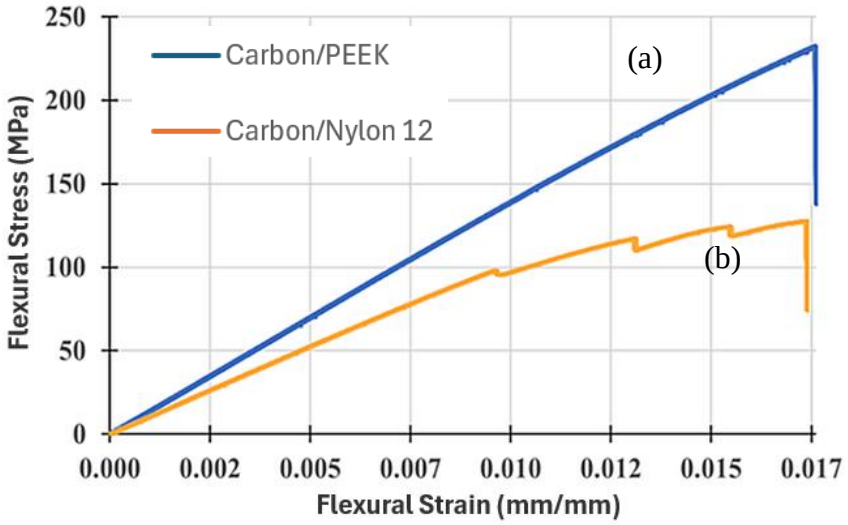

Figure 15: Flexural Stress-Strain Curve of (a) Carbon/PEEK and (b) Carbon/Nylon 12

Specimens predominantly exhibited shear failures at the midpoint, corresponding to regions of peak stress. Strain values were derived from crosshead displacement measurements. Given the central failure mode in the three-point flexural test, these values are expected to accurately represent actual maximum displacement. Carbon/PEEK showed a greater flexural modulus of 13.54 GPa and strength of 205.64 MPa compared to Carbon/Nylon 12 with a modulus of 11.36 GPa and strength of 128.81 MPa. Table 4 summarizes the properties of the flexural test.

Table 4: Flexural Stress-Strain Properties of Carbon/PEEK and Carbon/Nylon 12

Material	Flexural strength (MPa)	Flexural strain (%)	Flexural modulus (GPa)
Carbon/PEEK	205.6 ± 21.47	1.65 ± 0.052	13.54 ± 1.45
Carbon/Nylon 12	128.8 ± 8.94	1.82 ± 0.105	11.36 ± 0.18

4.4 Impact Test

Figures 16 and 17 show the front and back of the Carbon/PEEK and Carbon/Nylon 12 specimens, respectively. Indentations are clearly visible on the impact face of all tested specimens, but only the thinnest of each showed significant damage propagation through the back side of the specimens.

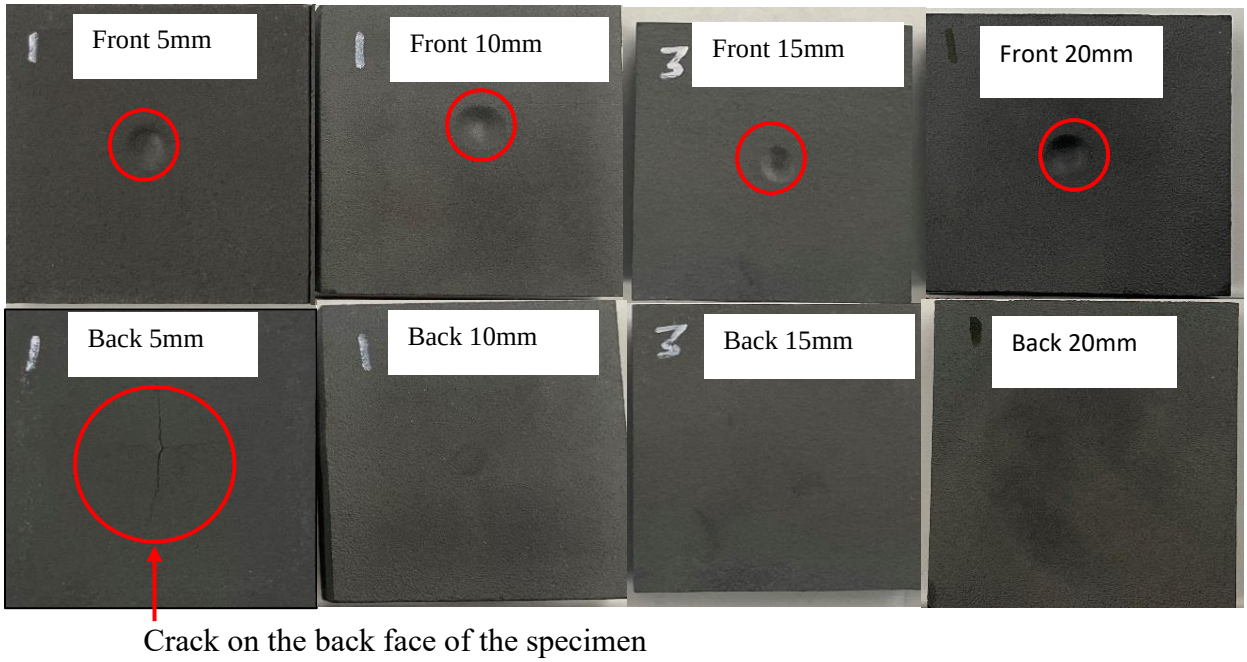

Figure 16: Carbon/Nylon 12 Tested Impact Specimens

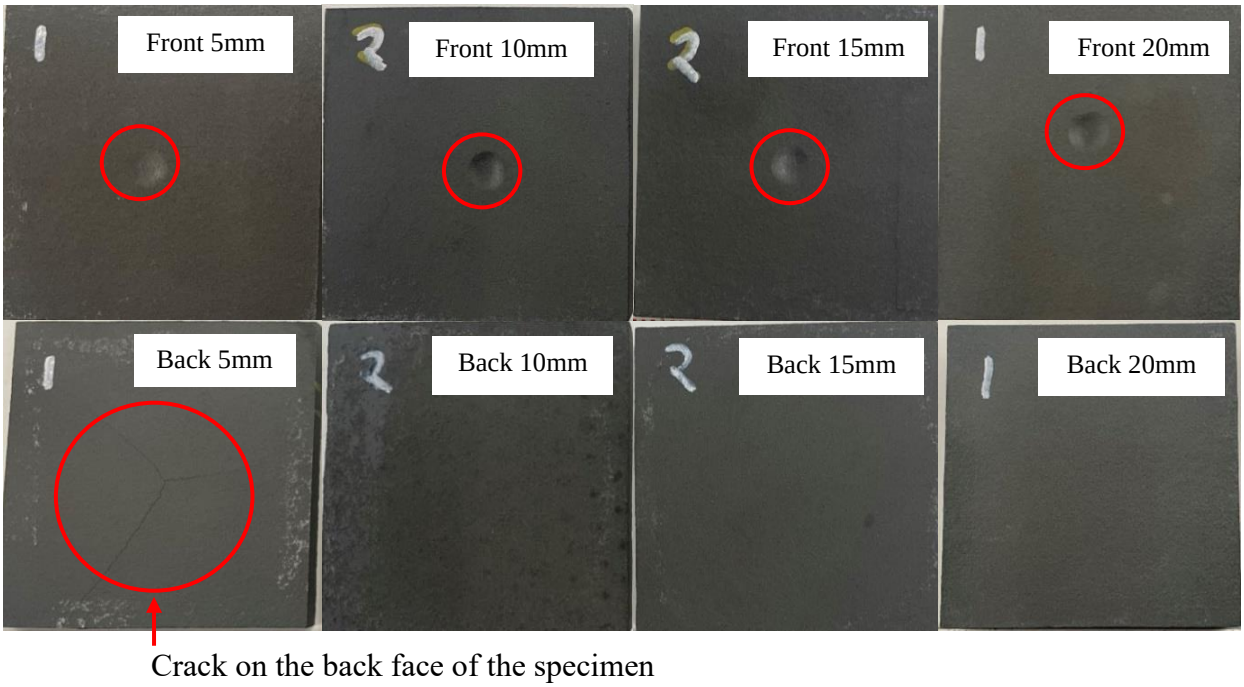

Figure 17: Carbon/PEEK Tested Impact Specimens

Figure 18 shows the Time vs. Energy curve of both the Carbon/PEEK and Carbon/Nylon 12 samples. The absorbed energy is represented by the vertical distance between the peak and settling point along the positive time axis. For Carbon/Nylon energy absorbed is directly proportional to material thickness. Carbon/PEEK displayed very similar energy absorption in all four thicknesses. Similar to Carbon/Nylon 12, stabilization time for the impactor was influenced by sample thickness.

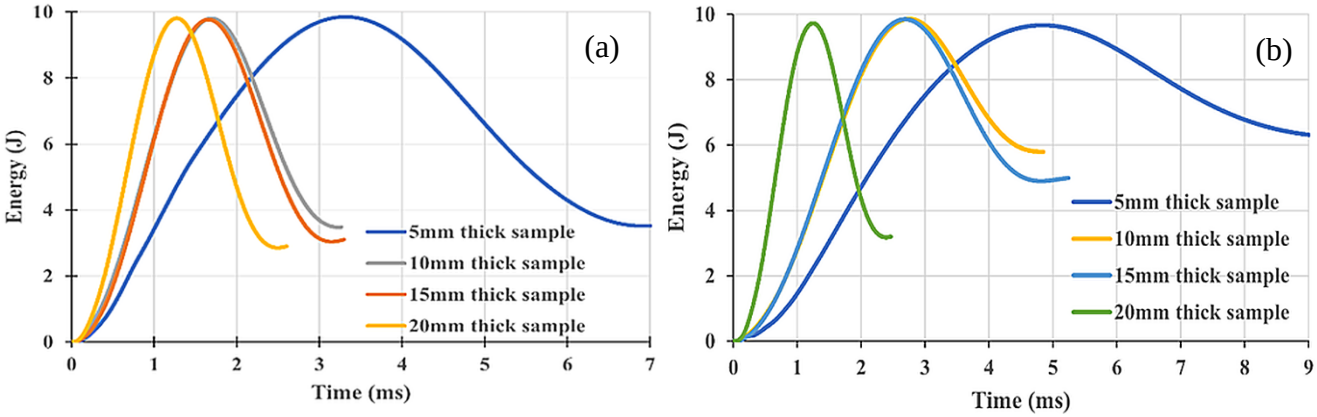

Figure 18: Time vs. Energy Curves of (a) Carbon/PEEK and (b) Carbon/Nylon 12

Thicker composite laminates absorbed greater impact energy not solely due to increased material thickness but also due to enhanced stiffness and greater interlaminar surface area, effectively distributing stresses, delaying crack propagation, and resisting delamination. For 5 mm specimens, the impactor required significantly more time to stabilize due to deeper penetration and resultant back-face cracking.

Table 5 shows the energy absorbed by the material for the 5mm, 10mm, 15mm, and 20mm for both the Carbon/PEEK and Carbon/Nylon 12. Carbon/PEEK consistently absorbed more impact energy across all thicknesses compared to Carbon/Nylon 12, demonstrating better energy dissipation capabilities. Notably, the absorbed energy for Carbon/PEEK increased only modestly from 6.12 J to 6.70 J despite a fourfold increase in thickness from 5 mm to 20 mm. This limited gain can be attributed to the high intrinsic toughness of the PEEK matrix, which enables efficient energy absorption even in thinner sections, leading to a saturation effect at higher thicknesses. Furthermore, the relatively high porosity and 2D random fiber orientation may constrain the benefits of additional material volume, limiting further improvement in damage tolerance with thickness [38]. This enhanced performance is likely attributable to PEEK's intrinsic toughness, providing superior resistance to crack propagation. In contrast, Carbon/Nylon 12 exhibited lower energy absorption especially in thinner samples, likely due to its lower matrix strength.

Table 5: Impact Properties of Carbon/PEEK and Carbon/Nylon 12

Characterization	Property	Carbon/PEEK	Carbon/Nylon 12
Impact Test	Absorbed Energy (J)	6.12 ± 0.31 (5 mm thick) 6.48 ± 0.48 (10 mm thick) 6.56 ± 0.79 (15 mm thick) 6.7 ± 0.16 (20 mm thick)	3.68 ± 0.17 (5 mm thick) 3.8 ± 0.13 (10 mm thick) 5.16 ± 0.17 (15 mm thick) 6.22 ± 0.49 (20 mm thick)

4.5 DSC/TGA Thermal Testing

Figure 19 shows the differential scanning calorimetry (DSC) and thermogravimetric analysis (TGA) of Carbon/PEEK in both the air and nitrogen environment. The TGA in Figure 19(a) depicts that degradation of the sample started at 350°C. The TGA in Figure 19(b) depicts decomposition starting at 375°C and the steps observed in mass change during heating are due to substances decomposing between 400°C and 500°C. The sample had a total mass loss of 4.62% before it reached its melting point. More residue was observed in the N_2 environment than in air. Thermal history of the polymer can be observed on both DSC curves at the 600°C mark and the melting point can be observed with a small peak at ≈350°C.

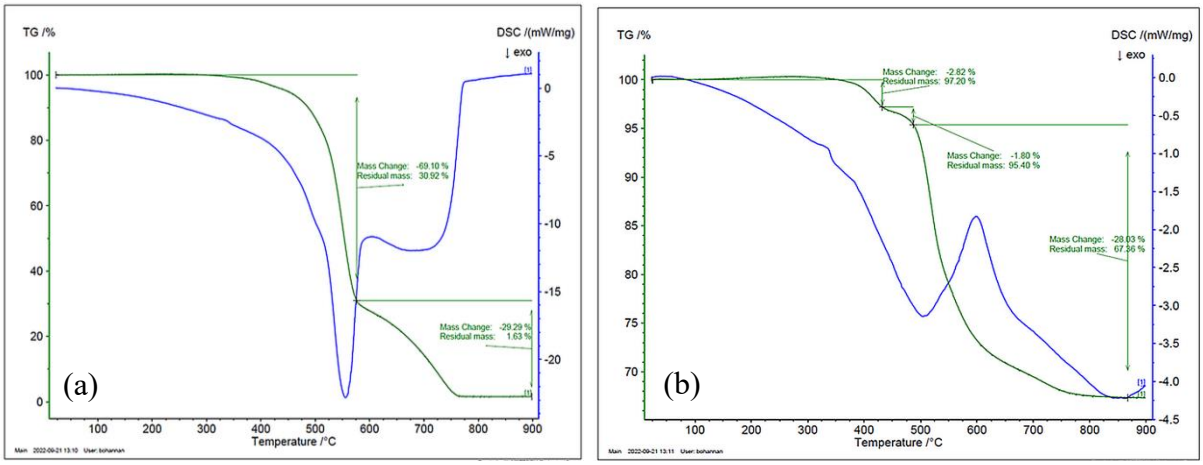

Figure 19: DSC and TGA of Carbon/PEEK in (a) Air and (b) Nitrogen Environment

Figure 20 shows the DSC and TGA of Carbon/Nylon 12 in both the air and nitrogen environment. From Figure 20(a) it can be observed that the degradation of the sample started at 298°C and the mass loss of 17.03% was observed between 298°C and 360°C. Total sample mass loss was 98.02% and 54.3% in an air and nitrogen environment, respectively. From Figure 20(b) it can be observed that more stability is observed in the nitrogen than in the air environment. In both environments, onset of melting can be seen in the DSC curve just before the 200°C mark. While multiple material transformations appear to occur continuously in the air environment, the DSC of the nitrogen

environment remains very linear, apart from a small bump at 400°C, which may be attributed to thermal history effects.

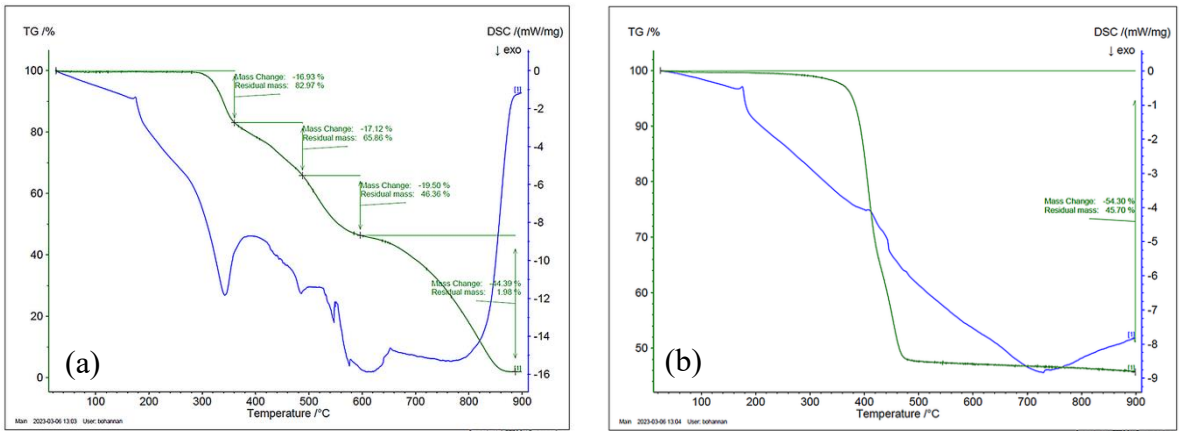

Figure 20: DSC and TGA of Carbon/Nylon 12 in (a) Air and (b) Nitrogen Environment

The thermal data provides context for both processing behavior and potential service conditions. The higher degradation onset temperature for Carbon/PEEK (~350°C) compared to Carbon/Nylon 12 (~298°C) suggests improved thermal stability, making it better suited for elevated temperature applications. The increased crystallization and melting temperatures in the Carbon/PEEK samples further reflect better heat resistance and dimensional stability. These trends are consistent with its overall mechanical performance and point to its suitability in environments where strength and thermal resistance are critical.

4.6 Discussion of Material Differences

The performance differences between Carbon/PEEK and Carbon/Nylon 12 are primarily due to differences in polymer structure, thermal stability, and fiber–matrix interaction. PEEK's rigid aromatic backbone gives it higher strength and stiffness, while Nylon 12's semi-crystalline structure makes it more flexible and lower in strength. This structural contrast explains the mechanical trends seen across tensile, flexural, and impact tests.

Thermal analysis showed that Carbon/PEEK begins degrading at a higher temperature (~350°C vs. ~298°C), making it better suited for elevated temperature applications. Compared to PEEK, Nylon 12's moisture sensitivity could reduce interfacial strength and overall performance. While elevated temperature mechanical testing wasn't completed in this study, Carbon/PEEK would be expected to outperform Carbon/Nylon 12 under elevated temperature mechanical loading.

The results indicate Carbon/PEEK composites are more suitable for high-performance applications, such as aerospace or automotive components requiring thermal and mechanical durability. Carbon/Nylon 12 composites are preferable for applications prioritizing cost-effectiveness, ease of processing, and moderate performance, including consumer products and interior components.

Compared to methods like FDM or injection molding, CBAM supports complex geometries with less tooling and shorter lead times. Although limited by current material availability and necessary post-processing steps, CBAM remains a robust manufacturing method for structural composites.

Conclusion

Carbon/PEEK and Carbon/Nylon 12 were additively manufactured using the CBAM process. The performance of the composites was evaluated based on mechanical tests and DSC/TGA testing. The following are some of the key outcomes of the tests conducted. Compressive strengths of Carbon/PEEK and Carbon/Nylon were both matrix dominated, both displaying strength approximately 60% of the respective pure polymeric strength. The tensile strength and elastic modulus of the Carbon/PEEK composite is 97.49% and 79.75% greater than the Carbon/Nylon composite. The flexural strength of Carbon/PEEK is 59.65% greater than the Carbon/Nylon. Carbon/PEEK also showed a higher energy absorption for all thickness variation (5mm, 10mm, 15mm, and 20mm) compared to Carbon/Nylon 12. Degradation of Carbon/PEEK began at a higher temperature compared to Carbon/Nylon (~350°C vs. ~298°C), but both displayed significant mass loss starting at 370°C.

This study highlights the potential of CBAM-fabricated composites in applications requiring high mechanical and thermal performance. Carbon/PEEK consistently outperformed Carbon/Nylon 12, but the current work is limited to in-plane loading and a fixed fiber/matrix system. Additional testing is needed to evaluate long-term durability, environmental exposure, and performance under multi-directional loading. Ongoing work is exploring alternate matrix materials and the use of unidirectional fiber mats to improve property consistency and expand application potential. These results support continued investigation of CBAM as a viable method for producing structural composite components.

Acknowledgments

This work was funded by the Department of Energy's Kansas City National Security Campus, which is operated and managed by Honeywell Federal Manufacturing & Technologies, LLC under contract number DE-NA0002839.

Data availability

The data that support the findings of this study are available from the corresponding author upon request.

Conflict of interest

The authors declare no competing interests.

References

1. Lupone, F., Padovano, E., Venezia, C., et al., “Experimental Characterization and Modeling of 3D Printed Continuous Carbon Fibers Composites with Different Fiber Orientation Produced by FFF Process”, *Polymers*, vol. 14, pp. 1-26, 2022.
2. Wu, H., Fahy, W., Kim, S., Kim, H., Zhao, N., Pilato, L., Kafi A., Bateman, S., and Koo, J. H., “Recent Developments in Polymers/Polymer Nanocomposites for Additive Manufacturing”, *Progress in Materials Science*, vol. 111 pp. 1-47, 2020.
3. Paesano, A., “Polymers for Additive Manufacturing: Present and Future”, *SAMPE Journal*, vol. 50, pp. 34-43, 2014.
4. Parandoush, P. and Lin, D., “A Review on Additive Manufacturing of Polymer-Fiber Composites”, *Composite Structures*, vol. 182, pp. 36-53, 2017.
5. Patel, R., Desai, C., Kushwah, S., and Mangrola, M., “A Review Article on FDM Process Parameters in 3D Printing for Composite Materials”, *Materials Today: Proceedings*, vol. 63, pp. 2162-2166, 2022.
6. Calignano, F., Manfredi, D., Ambrosio, E., Biamino, S., Lombardi, M., Atzeni, E., Salmi, A., Minetola, P., Iuliano, L., and Fino, P., “Overview on Additive Manufacturing Technologies”, *Proceedings of the IEEE*, vol. 105, pp. 593-612, 2017.
7. Parandoush, P., and Lin, D., “A Review on Additive Manufacturing of Polymer-Fiber Composites”, *Composite Structures*, vol. 182, pp. 36-63, 2017.
8. Taylor, G., Sudharshan, A., Murphy, D., Leu, M., and Chandrashekhara, K., “Fracture Toughness of Additively Manufactured Ultem 1010”, *Virtual and Physical Prototyping*, vol. 14, pp. 1-7, 2018.
9. Mani M., Lyons K. W., and Gupta S. K., “Sustainability Characterization for Additive Manufacturing”, *J Res Natl Inst Stand Technol*, vol. 119, pp. 419–428, 2014.
10. Cicala, G., Latteri, A., Del Curto, B., Russo, A., Recca, G., and Farè, S., “Engineering Thermoplastics for Additive Manufacturing: A Critical Perspective with Experimental Evidence to Support Functional Applications”, *Journal of Applied Biomaterials & Functional Materials*, vol. 15, pp. 10–18, 2017.
11. Wong, K. V., and Hernandez, A., “A Review of Additive Manufacturing”, *ISRN Mechanical Engineering*, vol. 2012, pp. 1–10, 2012.
12. Peeke, L. M., Liu, W., Periyasamy, M., Campbell, R. R., Sassano, E., Hajduczek, W. J., and Hickner, M. A., “Material Extrusion Additive Manufacturing of Dual Material Composite Thermoset Silicone Components”, *Polymer Engineering & Science*, vol. 64 pp. 218–230, 2023.
13. Setter, R., Riedel, F., Peukert, W., Schmidt, J., and Wudy, K., “Infiltration Behavior of Liquid Thermosets in Thermoplastic Powders for Additive Manufacturing of Polymer Composite Parts in a Combined Powder Bed Fusion Process”, *Polymer Composites*, vol. 42, pp. 5265–5279, 2021.

14. Lavernia, E., Shackelford, J., Zheng, B., Ma, K., and Schoenung, J., "Overview of Metal Additive Manufacturing Technologies", *Metallic Powders for Additive Manufacturing*, pp. 341–359, 2024. https://doi.org/10.1002/9781119908142.ch8
15. Withers, J. C., Loutfy, R. O., and Pickard, S. M., "Additive Manufacturing to Produce Standard and Custom Alloy Titanium", *Proceedings of the 13th World Conference on Titanium*, pp. 1413–1416, 2016.
16. Lakhdar, Y., Tuck, C., Binner, J., Terry, A., and Goodridge, R., "Additive Manufacturing of Advanced Ceramic Materials", *Progress in Materials Science*, vol. 116, 2021.
17. Margolis, J.M. "Engineering Thermoplastics: Properties and Applications", *CRC Press.* https://doi.org/10.1201/9781003066156
18. Griehl, W., and Djavid R. "Nylon-12 Preparation, Properties, and Applications." *Industrial & Engineering Chemistry* 62, vol. 62, pp. 16-22, 1970.
19. Kurtz, S. M., "Synthesis and Processing of Peek for Surgical Implants", *PEEK Biomaterials Handbook*, pp. 9–22, 2019. https://doi.org/10.1016/B978-1-4377-4463-7.10002-8
20. Barile, C., Casavola, C., and De Cillis, F., "Mechanical Comparison of New Composite Materials for Aerospace Applications", *Composites Part B: Engineering*, vol. 162, pp. 122–128, 2019.
21. Ma, C. C. M., Tai, N. H., Wu, S. H., Lin, S. H., Wu, J. F., and Lin, J. M. "Creep Behavior of Carbon-Fiber-Reinforced Polyetheretherketone (PEEK) [±45]4s Laminated Composites", *Composites Part B: Engineering*, vol. 28, pp. 407–417, 1997.
22. Hu, Y., Lin, Y., Yang, L., Wu, S., Tang, D., Yan, C., and Shi, Y., "Additive Manufacturing of Carbon Fiber-Reinforced Composites: A Review", *Applied Composite Materials*, vol. 31, pp. 353–398, 2024.
23. Yan, X., Yang, Y. and Hamada, H. "Tensile Properties of Glass Fiber Reinforced Polypropylene Composite and its Carbon Fiber Hybrid Composite Fabricated by Direct Fiber Feeding Injection Molding Process" *Polymer Composites*, vol. 39, pp. 3564-3574, 2018.
24. Zhang, D., D. Heider, S. G. Advani, and J. W. Gillespie, Jr., "Out of Autoclave Consolidation of Voids in Continuous Fiber Reinforced Thermoplastic Composites" *SAMPE*, 2013.
25. Bivens, C., Wood, A., Ruble, D., Rangapuram, M., Dasari, S. K., Chandrashekhara, K., and DeGrange, J. "Additively Manufactured Carbon Fiber- Reinforced Thermoplastic Composite Mold Plates for Injection Molding Process" *Appl Compos Materials*, vol. 30, pp. 1569–1586, 2023.
26. Liampas, S., Kladovasilakis, N., Tsongas, K., Pechlivani, E.M., "Recent Advances in Additive Manufacturing of Fibre-Reinforced Materials: A Comprehensive Review." *Applied Sciences*, https://www.mdpi.com/2076-3417/14/22/10100, vol. 14, pp. 1-22. 2024.

27. Barış Vatandaş, B., Uşun, A., Yıldız, N., Şimşek, C., Necati Cora, Ö., Aslan, M., & Gümrük, R. “Additive Manufacturing of peek-based continuous fiber reinforced thermoplastic composites with high mechanical properties.” *Composites Part A: Applied Science and Manufacturing*, vol. 167. https://doi.org/10.1016/j.compositesa.2023.107434 2023.
28. “Overview of Materials for Nylon 12” *MatWeb* Available: http://www.matweb.com/search/DataSheet.aspx?MatGUID=0e37a459c4eb452faa9d92659f9a0ccc
29. “Properties: Supplier Data - Polyetheretherketone (PEEK) (Goodfellow),” *AZoM* Available: https://www.azom.com/properties.aspx?ArticleID=1882
30. Kohutiar, M., Kakošová, L., Krbata, M., Janík, R., Fekiač, J.J., Breznická, A., Eckert, M., Mikuš, P., and Timárová, Ľ., "Comprehensive Review: Technological Approaches, Properties, and Applications of Pure and Reinforced Polyamide 6 (PA6) and Polyamide 12 (PA12) Composite Materials." *Polymers*, https://doi.org/10.3390/polym17040442 , vol. 17, pp. 1-40, 2025.
31. Weiler, S., Haffner, H.A., Chandrashekhara, K., Watts, J., Hilmas, G. E., Bayldon, J., and Rueschhoff, L.M., "Phenolic Polymer Infiltration and Pyrolysis Process for Additively Manufactured Carbon/PEEK Composites to Produce Carbon-Carbon Composites." *Progress in Additive Manufacturing*, https://doi.org/10.1007/s40964-024-00939-9, pp. 1-7, 2024.
32. “ASTM D6641: Standard Test Method for Compressive Properties of Polymer Matrix Composite Materials Using a Combined Loading Compression (CLC) Test Fixture”. ASTM Int. 2023.
33. “ASTM D7264: Standard Test Method for Flexural Properties of Polymer Matrix Composite Materials”. ASTM Int. 2015.
34. “ASTM D3039: Standard Test Method for Tensile Properties of Polymer Matrix Composite Materials”. ASTM Int. 2014.
35. “ASTM D7136: Standard Test Method for Measuring the Damage Resistance of a Fiber-Reinforced Polymer Matrix Composite to a Drop-Weight Impact Event”. ASTM Int. 2020.
36. Impossible Objects. *CBAM Composite Based Additive Manufacturing Process*. YouTube, 26 Apr. 2023. [Online]. Available: https://www.youtube.com/watch?v=uSOuv71IcFo
37. Wang, P., Zou, B. "Improvement of Heat Treatment Process on Mechanical Properties of FDM 3D-Printed Short- and Continuous-Fiber-Reinforced PEEK Composites." *Coatings*, https://www.mdpi.com/2079-6412/12/6/827 , vol. 12, pp. 1-14, 2022.
38. Eremin, A. V., Burkov, M. V., Bogdanov, A. A., Kononova, A. A., Lyubutin, P. S. “Impact Behavior and Residual Strength of PEEK/CF-Laminated Composites with Various Stacking Sequences.” *Polymers*, https://doi.org/10.3390/polym16050717, vol. 16, pp. 1-16. 2024.